Development/Plasticity/Repair

Ca^{2+} Influx through Mechanosensitive Channels Inhibits Neurite Outgrowth in Opposition to Other Influx Pathways and Release from Intracellular Stores

Bridget T. Jacques-Fricke,[1,2] **Yiqi Seow,**[3] **Philip A. Gottlieb,**[4] **Frederick Sachs,**[4] **and Timothy M. Gomez**[1,2]

[1]Department of Anatomy and [2]Neuroscience Training Program, University of Wisconsin, Madison, Wisconsin 53706, [3]Institute of Molecular and Cell Biology, Singapore, 138673, and [4]Department of Physiology and Biophysics, State University of New York at Buffalo, Buffalo, New York 14214

Ca^{2+} signals are known to be important regulators of neurite outgrowth and steering. Here we show that inhibiting Ca^{2+} influx through stretch-activated channels using various compounds, including a highly specific peptide isolated from *Grammostola spatulata* spider venom (GsMTx4), strongly accelerates the rate of neurite extension on diverse substrata and within the intact spinal cord. Consistent with the presence of stretch-activated channels, we show that Ca^{2+} influx is triggered by hypotonic solutions, which can be partially blocked by GsMTx4. Finally, chelating local, but not global, Ca^{2+} signals prevents the acceleration that is normally produced by GsMTx4. Blocking Ca^{2+} influx through other channel types has little or opposite effects, but release from intracellular stores is required for maximal acceleration. Together, our data suggest that Ca^{2+} functions at distinct microdomains in growth cones, with influx through mechanosensitive channels acting to inhibit outgrowth in opposition to influx through other plasma membrane channels and release from stores.

Key words: pathfinding; axon guidance; stretch activated channels; TRP; IP$_3$, ryanodine; spinal cord

Introduction

Many axon guidance cues regulate growth cone motility by triggering changes in intracellular Ca^{2+} concentration ([Ca^{2+}]$_i$) (for review, see Gomez and Zheng, 2006). Although studies of Ca^{2+} signaling have described multiple outcomes attributable to the amplitude, frequency, or localization of Ca^{2+} signals, the importance of the source of Ca^{2+} entry in the regulation of outgrowth is less clear. Coupling the site of Ca^{2+} entry with particular Ca^{2+} sensors is believed to provide some specificity for the diverse effects of Ca^{2+} on neuronal functions (Augustine et al., 2003). Ca^{2+} nanodomains (single channel) and microdomains (cluster of channels) are sites of Ca^{2+} entry that selectively activate Ca^{2+} effectors associated with the channel(s). However, the restricted spatial spread and short duration of some local Ca^{2+} signals makes them difficult to detect by standard fluorescence imaging techniques. Therefore, indirect approaches, such as the differential sensitivity to Ca^{2+} chelators BAPTA and EGTA, have been successfully used to infer local Ca^{2+} functions in synapses (Adler et al., 1991) and growth cones (Archer et al., 1999).

Ca^{2+} influx into growth cones occurs through voltage-operated and ligand-gated Ca^{2+} channels, as well as through several nontraditional Ca^{2+} channel types (Calabrese et al., 1999; Li et al., 2005; Shim et al., 2005; Wang and Poo, 2005). One particular channel type that is poorly understood in neurons is plasma membrane stretch-activated channels (SACs) (Sukharev and Anishkin, 2004; Kung, 2005). A role for SACs in the regulation of cell motility has been suggested in fish keratinocytes (Lee et al., 1999; Doyle et al., 2004; Doyle and Lee, 2005) and fibroblasts (Munevar et al., 2004). Although less well studied, Ca^{2+} influx through SACs has been suggested to negatively regulate axon outgrowth of leech neurons (Calabrese et al., 1999). However, the lack of specific blockers has made the study of SACs difficult. An important advance in the study of SACs came with the discovery and purification of a peptide from the tarantula *Grammostola spatulata* (GsMTx4), which appears to block SACs selectively (Suchyna et al., 2000, 2004).

Although Ca^{2+} influx through plasma membrane channels has diverse effects on growth cone motility (Mattson and Kater, 1987; Zheng et al., 1994), Ca^{2+} release from intracellular stores appears to promote outgrowth. For example, globally blocking Ca^{2+} release from IP$_3$ receptors reduces the rate of neurite elongation (Takei et al., 1998), whereas locally inhibiting (Hong et al., 2000; Xiang et al., 2002) or activating (Li et al., 2005) release promotes repulsive or attractive turning, respectively. Additionally, Ca^{2+} release through type 3 ryanodine receptors appears to support positive growth cone turning responses (Ooashi et al., 2005). Although growth-promoting effects have been attributed specifically to Ca^{2+} release from channels on intracellular stores, distinct effects of Ca^{2+} influx through different plasma membrane channels on neurite outgrowth have not been described.

In this study, we show that Ca^{2+} influx and release differentially regulate neurite outgrowth. We find that blockers of SACs dramatically accelerate axon extension both *in vitro* and *in vivo*, suggesting that influx through SACs normally suppresses out-

growth. Maximal acceleration of neurite outgrowth by SAC blockers requires Ca^{2+} influx through other plasma membrane channels and release from intracellular stores, suggesting that these Ca^{2+} signaling pathways support outgrowth. Moreover, the ability of GsMTx4 to stimulate neurite extension is prevented by fast, but not slow, Ca^{2+} chelators. Together, these results suggest that multiple functional Ca^{2+} signals, including influx through SACs and release from intracellular stores, operate within distinct nanodomains or microdomains to inhibit or promote neurite outgrowth.

Materials and Methods

Xenopus spinal cord explant cultures. Spinal cords were dissected from stage 22–25 *Xenopus* embryos, and explants were plated on acid-washed glass coverslips coated with 10 μg/ml fibronectin (FN) (Sigma, St. Louis, MO) or laminin (LN) (Sigma) or 100 μg/ml poly-D-lysine (PDL) (Sigma) as described previously (Gomez et al., 2003). Cultures were imaged 16–24 h after plating. Mounting explant cultures in perfusion chambers as described previously (Gomez et al., 2003) allowed for rapid exchange of solutions.

In vitro *imaging and analysis.* The rate of axon outgrowth was analyzed from phase-contrast time-lapse images collected with a Zeiss (Thornwood, NY) Axiovert microscope and a 20× objective. Images were captured with a Coolsnap HQ digital camera (Roper Scientific, Trenton, NJ) at 1 min intervals for at least 15 min in control solution and an additional 30 min after experimental manipulations. MetaMorph software (Universal Imaging Corporation, Sunnyvale, CA) was used for acquisition and analysis. Ca^{2+} influx and release pathways were inhibited using gentamicin (Sigma), gadolinium (Gd^{3+}) (Sigma), ruthenium red (Tocris Bioscience, Ellisville, MO), 2-aminoethoxy-diphenylborate (2APB) (Calbiochem, La Jolla, CA), thapsigargin (Biomol, Plymouth Meeting, PA), ryanodine (Calbiochem), and GsMTx4. The linear peptide GsMTx4 was chemically synthesized (SynPep, Dublin, CA). Folding was achieved as described previously (Ostrow et al., 2003). Purity was assessed by analytical reverse-phase HPLC and mass spectrometry and was generally >98%. To chelate intracellular Ca^{2+}, BAPTA-AM and EGTA-AM (Calbiochem) were loaded for 1 h before imaging. Statistical significance was determined with either Student's or Mann–Whitney *t* tests by InStat software (GraphPad Software, San Diego, CA), with variance reported as ±SEM.

In vivo *imaging.* For fluorescence imaging of neurons in vivo, 0.85 ng of in vitro transcribed, capped green fluorescent protein (GFP) mRNA (mMessage Machine; Ambion, Austin, TX) was injected into one blastomere of eight-cell stage embryos. Stage 22–24 embryos were pinned laterally onto a Sylgard dish and dissected in ~1 mg/ml collagenase B in modified Ringer's (MR) solution. The skin and somites were removed from one side of the embryo to expose the spinal cord. Dissected embryos were rinsed extensively with MR solution before imaging. To reduce solution volume, a glass ring was sealed with vacuum grease around the pinned embryo. GFP fluorescence images were collected at 15 s intervals with a 20× water objective on an Olympus (Tokyo, Japan) Fluoview 500 laser-scanning confocal system. After a 15 min control period, GsMTx4 was applied to a final concentration of 5 μM. MetaMorph software was used for analysis.

Isotonic and hypotonic solutions. Normal MR solution containing (in mM) 100 NaCl, 2 KCl, 2 CaCl$_2$, 1 MgCl$_2$, and 5 HEPES was modified to create isotonic and hypotonic solutions. For isotonic MR solution, NaCl was reduced to 50 mM and 100 mM D-mannitol was added, whereas hypotonic MR solution was identical to the isotonic solution except D-mannitol was omitted. Osmolality of the solutions was determined with an Advanced Osmometer (model 3D3; Advanced Instruments, Norwood, MA) using the freezing-point method. The osmolality of isotonic solution was 219.7 ± 0.6 mOsm/kg and hypotonic solution was 119.0 ± 0 mOsm/kg (averages of three readings), creating a 46% hypotonic solution. The pH of all solutions was adjusted to 7.6.

Ca^{2+} imaging and analysis. To examine intracellular Ca^{2+} concentration during osmotic changes, neurons were loaded with cell-permeant fura-2 AM (2.5 μM; Invitrogen, Carlsbad, CA) for 15–30 min. Fluores-

cent images excited at 340 and 380 nm were captured at 30 s intervals with a 40× Fluorite objective (numerical aperture, 1.4) on a Zeiss Axiovert microscope. MetaFluor software was used for image acquisition and analysis. Ratio measurements were made from background-subtracted images using cell-free regions as background. Measurements of baseline Ca^{2+} changes were made with fura-2 AM loaded as above or FFP-18 (fura-piperazine-C$_{12}$H$_{25}$) AM (2.5 μM; TEF Labs, Austin, TX) loaded for 2 h. To measure Ca^{2+} release from intracellular stores, neurons were loaded with cell-permeant Fluo-4 AM (2.0 μM; Invitrogen) in 0.01% pluronic acid for 45 min. Images were collected at 5 s intervals with a 60× PlanApo objective (numerical aperture, 1.45) on an Olympus Optical Fluoview 500 laser-scanning confocal mounted on an AX-70 upright microscope. m-3M3FBS [2,4,6-trimethyl-N-(m-3-trifluoromethyl-phenyl)benzenesulfonamide] (Calbiochem) was added to activate phospholipase C (PLC). Ca^{2+} elevations were regarded as significant if the average Fluo-4 intensity increased ≥10% over baseline (2 SDs above noise) after addition of PLC activator. Fluoview software was used for image acquisition and analysis. The average rate increase over pretreatment rate was used to calculate the half-maximally effective dose of GsMTx4 using Prism 4 software (GraphPad Software). Statistical significance was determined with either Student's or Mann–Whitney *t* tests using InStat software (GraphPad Software) with variance reported as ±SEM.

Results

Reducing Ca^{2+} influx through SACs accelerates neurite outgrowth

To assess how Ca^{2+} influx pathways regulate neurite outgrowth, we blocked Ca^{2+} influx by several specific and nonspecific means and observed the acute effects on growth cone motility using time-lapse microscopy. Consistent with previous reports (Holliday et al., 1991; Gu and Spitzer, 1995), blocking or reducing all Ca^{2+} influx through plasma membrane channels by eliminating or significantly lowering extracellular Ca^{2+} concentration led to an immediate twofold acceleration in the rate of neurite outgrowth (199.6 ± 17.4 and 187.0 ± 26.2% of control growth rate for elimination or reduction of extracellular Ca^{2+}; $n = 67$ and 29, respectively) (Fig. 1a). Similarly, blocking influx with Gd^{3+}, a general Ca^{2+} channel blocker, causes a comparable increase in neurite extension rate (184.8 ± 25.0% of control growth rate; $n = 49$) (Fig. 1a). Because Gd^{3+} potently blocks SACs (Hamill and McBride, 1996), we tested gentamicin, another blocker of mechanosensitive channels. Gentamicin is typically present in our culture media at a concentration of 100 μM as an antibiotic. Therefore, to test whether gentamicin influenced the rate of neurite extension, we doubled the normal concentration of gentamicin to 200 μM. We found that addition of two times gentamicin increased neurite growth rates similar to 0 Ca^{2+} and Gd^{3+} (190.2 ± 33.2% of control growth rate; $n = 31$) (Fig. 1a). Consistent with gentamicin acting as a Ca^{2+} influx blocker, we found that removing all aminoglycoside antibiotics (gentamicin and streptomycin) from cultured neurons led to an immediate increase in spontaneous Ca^{2+} transient activity in growth cones (supplemental Fig. 1, available at www.jneurosci.org as supplemental material). Because gentamicin may also have nonselective effects on Ca^{2+} influx (Hamill and McBride, 1996), we obtained a highly selective peptide blocker of SACs isolated from *Grammostola spatulata* spider venom (GsMTx4) (Suchyna et al., 2000, 2004). Interestingly, addition of GsMTx4 to cultured neurons resulted in significantly greater acceleration of neurite extension compared with all other influx blockers tested (Fig. 1a) (supplemental video 1, available at www.jneurosci.org as supplemental material). Although less selective manipulations of Ca^{2+} influx caused an approximate doubling in average extension rate, neurites exposed to GsMTx4 grew on average 3.5 times faster than

their pretreatment growth rates (349.1 ± 19.3% of control growth rate; $n = 101$) (Fig. 1a). After a brief delay, accelerated outgrowth was partially reversed on peptide washout (Fig. 1c). Together, these results suggest that the GsMTx4 peptide selectively blocks an open channel that slows axon outgrowth when active. Moreover, because less selective treatments are significantly less effective in stimulating neurite extension than GsMTx4, it appears that influx through some plasma membrane channels may normally support outgrowth. These results also indicate that these different channel types are normally highly active on growth cones extending on FN in culture.

In addition to testing blockers of SACs, we also tested blockers of transient receptor potential (TRP) channels because some of these channels are known to be mechanosensitive (Lin and Corey, 2005). Ruthenium red, which blocks TRPV (TRP vanilloid receptor) channels (Watanabe et al., 2002; Patapoutian et al., 2003), stimulated neurite extension similarly to less selective treatments and significantly less than GsMTx4 (246.0 ± 20.6% of control growth rate; $n = 44$) (Fig. 1a). Although ruthenium red is known to block ryanodine receptors, it is not cell permeant, so the effects of bath application should be limited to plasma membrane channels (Tani and Ametani, 1971; Korte and Rosenbluth, 1982). Conversely, SKF-96365 [1–2-(4-methoxyphenyl)-2-[3-(4-methoxyphenyl)propoxy]ethyl-1H-imidazole] significantly slowed neurite outgrowth on FN (26.5 ± 21.6% of control growth rate; $n = 36$) (Fig. 1a). Although SKF-96365 has nonspecific effects on other channel types (Merritt et al., 1990; Schwarz et al., 1994), it has been used extensively in the study of TRPC (classical TRP) channels (Li et al., 1999, 2005; Kim et al., 2003; Shim et al., 2005; Wang and Poo, 2005). These results suggest that growth cones express multiple TRP channels that may have opposing effects on neurite extension. Finally, whereas a mixture of voltage-operated Ca²⁺ channel (VOCC) blockers had no significant effect on neurite growth rate (126.6 ± 18.3% of control growth rate; $n = 58$) (Fig. 1a), Cd²⁺, a general channel blocker, inhibited neurite outgrowth (41.3 ± 14.9% of control growth rate; $n = 22$) (Fig. 1a). Together, these results suggest that different Ca²⁺ influx pathways have opposing effects on neurite extension. Acceleration of outgrowth in response to Gd³⁺, gentamicin, and GsMTx4 implicates SACs in the inhibition of outgrowth, whereas channels blocked by SKF-96365 and Cd²⁺ appear to promote outgrowth.

GsMTx4 stimulates neurite outgrowth over diverse substrata in vitro and in the intact spinal cord

Blocking SACs immediately accelerates axon extension by neurons on the extracellular matrix protein FN, suggesting that SACs are constitutively active on growth cones on this substratum. To test whether SACs modulate outgrowth on other substrata, we
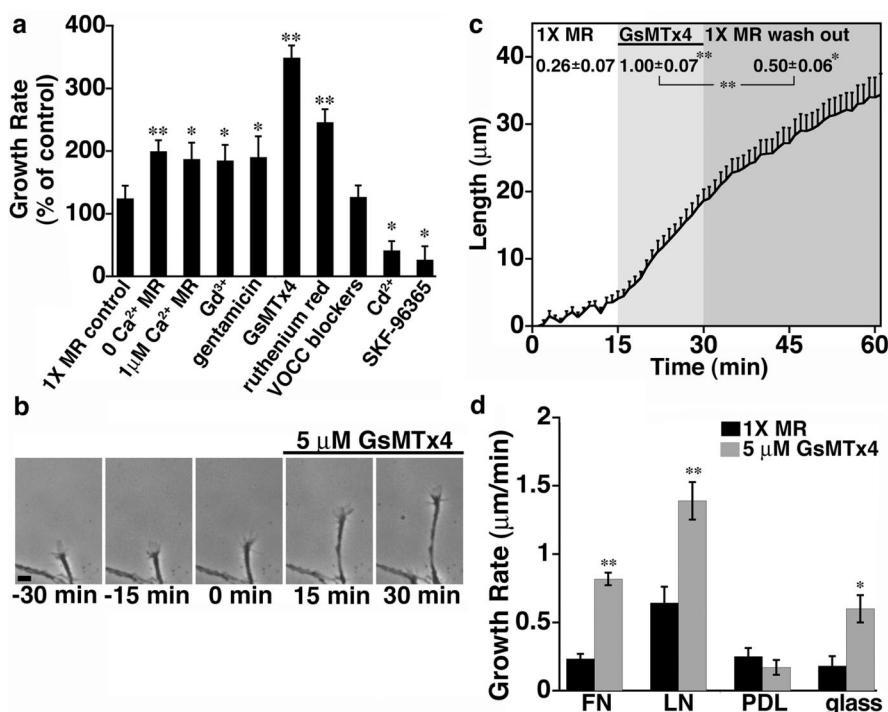

Figure 1. Reducing Ca²⁺ influx through SACs increases neurite growth rates. **a**, Change in the average rate of neurite outgrowth during the 15 min period after various Ca²⁺ influx manipulations. Ca²⁺ influx was eliminated or reduced with 0 or low extracellular Ca²⁺ or blocked using Gd³⁺ (100 μM), gentamicin (200 μM), GsMTx4 (5 μM), ruthenium red (1 μM), a mixture of blockers for voltage-operated Ca²⁺ channels (1 μM ω-conotoxin, 100 nM nifedipine, 50 μM NiCl, and 60 nM ω-agatoxin), Cd²⁺ (50 μM), and SKF-96365 (3 μM). Each condition was normalized to the 15 min period preceding exposure to Ca²⁺ changes or blockers. Unless specified, each condition was presented in 1× MR solution (with 2 mM Ca²⁺ and 100 μM gentamicin). **b**, Representative images of an individual Xenopus spinal neuron axon at 15 min intervals before and after application of GsMTx4. Scale bar, 10 μm. **c**, The length of axons over a 60 min observation period before treatment (white shading), in the presence of 5 μM GsMTx4 (light shading), and after peptide washout (dark shading). For this graph, analysis was limited to responsive neurons (increased growth rate by at least 200%; $n = 10$ neurites). The average rates of outgrowth (micrometer per minute) during each period are shown above the corresponding graph. Similar results were found for all neurites tested (before treatment, 0.25 ± 0.04 μm/min; GsMTx4, 0.73 ± 0.05 μm/min; washout, 0.42 ± 0.05 μm/min; $n = 67$). **d**, Average rates of outgrowth 15 min before and after addition of GsMTx4 to neurons growing on different substrata. Blocking SACs with GsMTx4 significantly accelerates outgrowth on FN, LN, and glass but not on PDL. All averages are reported ±SEM. *$p < 0.05$; **$p < 0.001$. $n \geq 22$ for all conditions.

tested the effects of GsMTx4 on the rate of neurite outgrowth by neurons extending on different substrata. On laminin, another potent growth-promoting extracellular matrix protein, GsMTx4 enhances neurite extension but to a lesser degree than FN because of higher baseline rate of outgrowth on LN (216.3 ± 21.4% of control growth rate; $n = 29$) (Fig. 1d). To determine whether this is an integrin-dependent process, we tested the effects of GsMTx4 on neurons cultured on PDL and glass. Whereas GsMTx4 does not increase the rate of outgrowth on PDL, blocking SACs does accelerate neurite extension on glass. These results suggest that active SACs limit neurite extension on several unrelated substrata and that channel activity does not depend on integrin engagement (although the degree of SAC activity could be modulated by the substrata). It is not clear whether SACs are inactive on neurites extending on PDL or whether blocking these channels cannot be converted into increased growth rates. Because the growth-promoting effect of GsMTx4 is most significant on FN, we chose to focus on this substratum for the remaining in vitro experiments.

To determine whether SACs also limit axon extension in vivo, we imaged GFP-labeled neurons in the developing Xenopus spinal cord (Fig. 2) (supplemental video 2, available at www.jneurosci.org as supplemental material). Time-lapse confocal
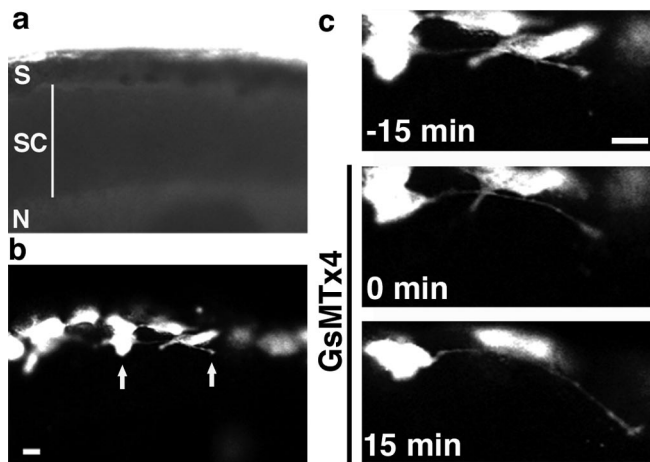
Figure 2. Reducing Ca^{2+} influx through SACs with GsMTx4 increases neurite growth rates *in vivo*. **a**, Bright-field image of an embryo with skin and somites removed for *in vivo* confocal imaging. Dorsal is up, and anterior is to the left. S, Skin; SC, spinal cord; N, notochord. **b**, Fluorescence image of this embryo with GFP-labeled cells in the skin and dorsal spinal cord. Arrows indicate the cell body and growth cone of an extending axon. **c**, Time-lapse images of the labeled neuron in **b** at 15 min intervals before and after bath application of 5 μM GsMTx4. Scale bars, 20 μm.

images of spinal axons extending within an exposed cord preparation (Gomez and Spitzer, 1999) were examined before and after addition of GsMTx4. As observed *in vitro*, the average rate of neurite extension increased after the addition of GsMTx4 (0.57 ± 0.09 μm/min before GsMTx4 addition; 0.96 ± 0.13 μm/min after GsMTx4 addition; $p < 0.05$), suggesting that influx through a mechanosensitive channel inhibits outgrowth of spinal neurites *in vivo*. Although the majority of axons examined were oriented longitudinally in the spinal cord (16 of 23), increased outgrowth in response to GsMTx4 was observed in both longitudinal axons (primarily Rohon-Beard and motoneurons) and commissural interneurons, suggesting a general mechanism for regulation of neurite outgrowth *in vivo*.

Xenopus spinal neurites express SACs that are blocked by GsMTx4

Based on the stimulatory effects that several pharmacological SAC blockers have on motility, growth cones appear to express a mechanosensitive channel. However, because the effects on motility are an indirect readout of a complex process, we sought a more direct measure of SAC activity on growth cones. For this, we stimulated membrane stretch with hypotonic solution while imaging [Ca^{2+}]$_i$ with fura-2 to test whether GsMTx4-sensitive Ca^{2+} influx is activated in growth cones during cell swelling. Because fura-2 is a two-excitation wavelength Ca^{2+} indicator, ratio images (340 and 380 nm) control for potential artifacts attributable to cell swelling. Stimulation of neurons with a 46% hypotonic solution caused a brief transient Ca^{2+} elevation followed by tonically elevated [Ca^{2+}]$_i$ (>10% ratio change over baseline) in a majority of growth cones tested (89%; $n = 128$) (Fig. 3). This is similar to Ca^{2+} signaling patterns observed previously in neurons (Viana et al., 2001). To test whether hypotonically induced Ca^{2+} signals were sensitive to blockers that accelerate outgrowth, GsMTx4 or gentamicin were added during the tonic phase of osmotic stretch. We find that [Ca^{2+}]$_i$ was immediately reduced by both GsMTx4 and gentamicin, suggesting that SACs were partially blocked (Fig. 3a,c). The inability of GsMTx4 and gentamicin to completely block stretch-activated influx is

likely attributable to the overwhelming nature of stretch produced by hypotonic stimulation, which would maximally activate all SACs. To determine whether other channels contributed to tonic phase Ca^{2+} influx in hypotonic solution, we tested a mixture of VOCC blockers. Ca^{2+} influx through VOCCs has been shown to contribute to the response to hypotonic solution in cultured mouse primary sensory neurons (Viana et al., 2001). However, we found that VOCC blockers had little effect on [Ca^{2+}]$_i$ during cell swelling, suggesting that influx through VOCCs does not contribute to the Ca^{2+} response in hypotonic solution. These data suggest that *Xenopus* spinal neurons express Ca^{2+}-permeable SACs that can be blocked by gentamicin and GsMTx4.

Ca^{2+} influx through different plasma membrane channels has opposing functional effects on neurite outgrowth

To further test the specificity of GsMTx4 as a Ca^{2+} channel blocker and to begin to distinguish the functional effects of different channel activities, we examined the response of neurites to GsMTx4 in various extracellular Ca^{2+} conditions. If GsMTx4 acts by blocking a Ca^{2+}-permeable channel, then it should require more blocker to accelerate neurite outgrowth when the driving force for Ca^{2+} influx is increased by higher extracellular Ca^{2+} concentration. We examined the dose–response effects of GsMTx4 in 2 and 10 mM extracellular Ca^{2+}. First, in normal Ca^{2+} MR solution (2 mM), the effects of GsMTx4 were dose dependent and saturable with a half-maximal dose of ~2.6 μM (see Materials and Methods). However, when extracellular Ca^{2+} concentration was elevated to 10 mM, GsMTx4 could not stimulate outgrowth as effectively (Fig. 4a). This is consistent with an incomplete block of Ca^{2+} influx through SACs at 5 μM GsMTx4.

Blocking Ca^{2+} influx through SACs with GsMTx4 accelerates neurite outgrowth significantly more than less specific treatments, such as Ca^{2+}-free media, which eliminates all influx. This result suggests that influx through some channels promotes outgrowth in opposition to influx through GsMTx4-sensitive SACs, which inhibits outgrowth. To test whether maximal acceleration in response to GsMTx4 depends on continued Ca^{2+} influx through other plasma membrane channels, we applied GsMTx4 in 0 extracellular Ca^{2+}. GsMTx4 does not potentiate neurite outgrowth in 0 Ca^{2+} above the acceleration seen with 0 Ca^{2+} solution alone (Fig. 4b). This result is consistent with the notion that GsMTx4 stimulates neurite outgrowth by decreasing Ca^{2+} influx through selective channel(s) but that maintained Ca^{2+} influx through other channels is necessary for maximal outgrowth. Because blocking Ca^{2+} influx with Cd^{2+} and SKF-96365 slows rather than stimulates outgrowth (Fig. 1a), it is likely that these inhibitors more selectively block channels that support neurite extension rather than growth-inhibiting SACs. If true, then simultaneous addition of GsMTx4 with SKF-96365 should lead to intermediate outgrowth rates. Indeed, we find that GsMTx4 together with SKF-96365 stimulates neurite extension similar to 0 Ca^{2+} MR alone (Fig. 4b). Together, these data suggest that Ca^{2+} influx through specific plasma membrane channels can either promote outgrowth (TRPC channels) or inhibit growth rates (SACs).

GsMTx4 inhibits local Ca^{2+} signaling

Although our data suggest that reduced Ca^{2+} influx is responsible for the growth-promoting effects of GsMTx4, we cannot detect changes in baseline [Ca^{2+}]$_i$ within growth cones in response to GsMTx4 using either cytosolic or near-membrane fura-2 Ca^{2+} indicators (supplemental Fig. 2, available at www.jneurosci.org

as supplemental material). Whereas GsMTx4 does not decrease the average $[Ca^{2+}]_i$, highly localized Ca^{2+} changes may be responsible for the robust and immediate behavioral effects of blocking SACs. This result would be consistent with the literature showing local Ca^{2+} microdomains that couple open channels with downstream Ca^{2+} effectors (Archer et al., 1999; Augustine et al., 2003).

To investigate the possibility that GsMTx4 inhibits local Ca^{2+} signals, we compared the effects of the Ca^{2+} buffers BAPTA and EGTA on growth acceleration induced by GsMTx4. Although BAPTA and EGTA have similar equilibrium affinities for Ca^{2+}, the binding rate of BAPTA is 50–400 times faster than EGTA (Tsien, 1980). Previous studies examining Ca^{2+} microdomains have demonstrated that intracellular BAPTA chelates Ca^{2+} fast enough to reduce local Ca^{2+} elevation and activation of effectors, whereas EGTA allows local signaling to persist (Augustine et al., 2003) (schematized in supplemental Fig. 3, available at www.jneurosci.org as supplemental material). As predicted, loading neurons with BAPTA-AM blocked the growth-promoting effects of GsMTx4 (Fig. 5). Conversely, neurite extension by neurons loaded with a high concentration of EGTA-AM accelerated significantly in response to GsMTx4. These data suggest that Ca^{2+} influx through a mechanosensitive channel acts within a Ca^{2+} microdomain that is buffered by BAPTA but not EGTA. GsMTx4 cannot stimulate neurite outgrowth in the presence of BAPTA because all Ca^{2+} signals, including Ca^{2+} near channel pores, have been buffered so blocking Ca^{2+} influx has no additional effect. Surprisingly, BAPTA alone does not stimulate neurite extension as occurs with elimination of extracellular Ca^{2+}. This could be attributable to the effective buffering of all influx signals, those inhibiting and supporting growth, as well as buffering at sites of Ca^{2+} release from intracellular stores, which have been shown to support neurite extension (Takei et al., 1998; Brailoiu et al., 2005; Ooashi et al., 2005) (Fig. 6).

Ca^{2+} release from intracellular stores supports neurite outgrowth and is required for maximum growth after blocking mechanosensitive influx

Inhibiting Ca^{2+} influx with treatments of varying channel specificity results in differences in both the rate and persistence of increased outgrowth. When extracellular Ca^{2+} is removed (the least specific treatment), the increased rate of neurite outgrowth is temporary, lasting 13 min before a return to normal growth rate (Fig. 6a). Conversely, gentamicin and GsMTx4 stimulate neurite outgrowth that persists for longer than 30 min (Fig. 6a). One possible explanation for the difference in the duration of the effect is that intracellular Ca^{2+} stores are depleted after prolonged exposure to 0 Ca^{2+} MR, whereas stores remain intact in gentamicin and GsMTx4. To test this hypothesis, we imaged
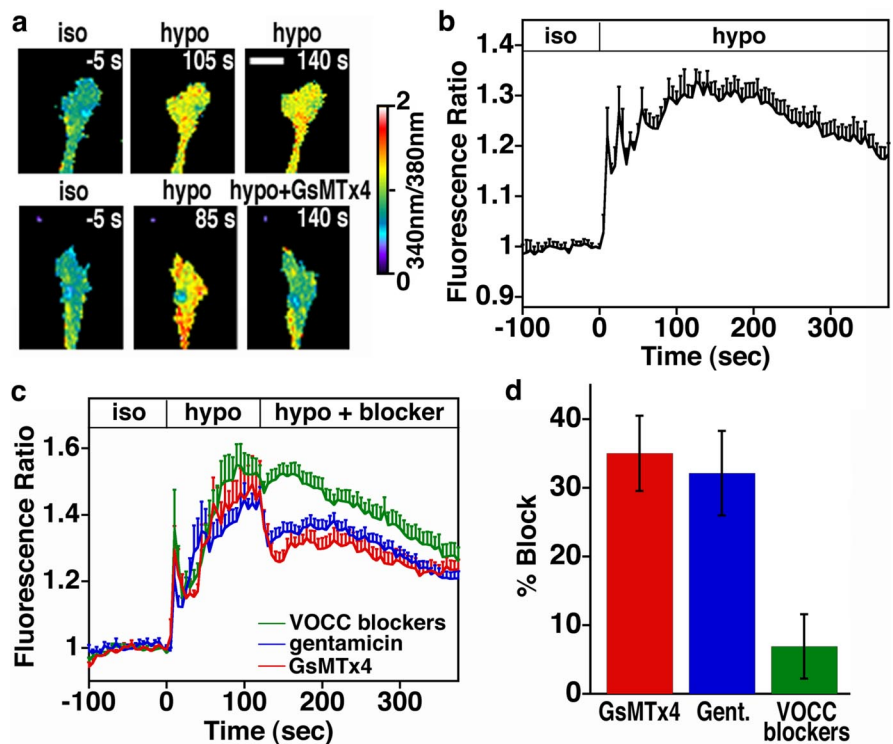

Figure 3. Ca^{2+} influx through SACs on *Xenopus* spinal neurons is activated by membrane stretch with hypotonic solution and inhibited with SAC blockers. *a*, Pseudocolored fluorescence ratio images of fura-2-loaded growth cones exposed to osmotic stretch with hypotonic solution. Growth cones were shifted from isotonic (iso) to hypotonic (hypo) solution at 0 s. In bottom row, after 120 s in hypotonic solution, SACs were blocked with 5 μM GsMTx4. Scale bar, 10 μm. *b*, Average fura-2 fluorescence ratio over time measured within growth cones exposed to a 46% hypotonic solution. Ca^{2+} transients followed by tonic Ca^{2+} elevations were typically observed. *c*, Average fura-2 fluorescence ratio over time measured within growth cones exposed to a 46% hypotonic solution followed by Ca^{2+} channel blockers [5 μM GsMTx4, 200 μM gentamycin, or a mixture of VOCC blockers (1 μM ω-conotoxin, 100 nM nifedipine, 50 μM NiCl, and 60 nM ω-agatoxin)] during the tonic phase. Data in *b* and *c* were normalized to the fluorescence ratio in isotonic solution immediately before addition of hypotonic solution. *d*, The average reduction in fura-2 fluorescence ratio (percentage of pretreatment) caused by each blocking condition measured at the point of maximum inhibition 5–25 s after application of each blocker. Only growth cones that exhibited a significant increase in Ca^{2+} (≥10% over baseline) after addition of hypotonic solution were included in this analysis. $n \geq 21$ for all conditions. Gent, Gentamicin.

$[Ca^{2+}]_i$ in growth cones loaded with Fluo-4 while stimulating store release with *m*-3M3FBS, a PLC activator. Activation of PLC stimulates IP$_3$ production, which triggers Ca^{2+} release through IP$_3$ receptors on intracellular stores. We used the amplitude of Ca^{2+} transients resulting from IP$_3$-mediated Ca^{2+} release as a readout of the Ca^{2+} content within intracellular stores. *m*-3M3FBS was administered in 0 Ca^{2+} MR to ensure that the Ca^{2+} transient was solely attributed to store release and not influx resulting from PLC activation. We compared the peak amplitude of Ca^{2+} transients from growth cones in normal media (with 2 mM Ca^{2+}) to growth cones pretreated with 0 Ca^{2+} MR, gentamicin, or GsMTx4 for 5 or 15 min (Fig. 6b). When Ca^{2+} is released from IP$_3$-sensitive stores immediately on shifting to 0 extracellular Ca^{2+}, a large Ca^{2+} transient is observed in a majority of growth cones (Fig. 6b, inset), indicating that stores are typically well loaded with Ca^{2+}. In contrast, when extracellular Ca^{2+} is eliminated for 15 min before PLC activation, most growth cones have no response, and, of those responding, there was only a low-amplitude Ca^{2+} transient, suggesting that the stores were depleted. Conversely, growth cones pretreated with the SAC blockers gentamicin or GsMTx4 for 15 min still exhibit high-amplitude Ca^{2+} transients during PLC activation, indicating that the stores remain well loaded. The correlation between
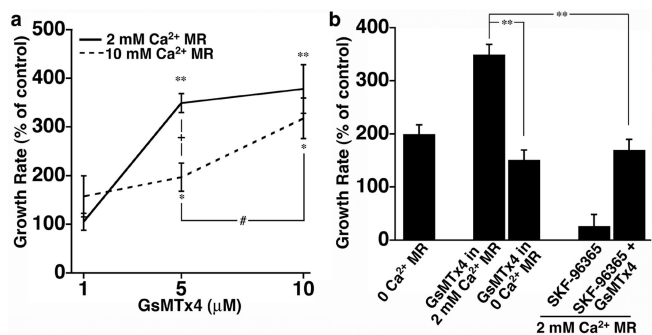
Figure 4. Ca^{2+} influx through different plasma membrane channels has opposite effects on neurite outgrowth. ***a***, Dose–response curve for GsMTx4 effect on rate of outgrowth in 2 and 10 mM Ca^{2+} MR solution. GsMTx4 is less effective at higher extracellular Ca^{2+} but still has a dose-dependent effect on outgrowth. *$p < 0.05$, **$p < 0.001$ compared with pretreatment control; $^+p < 0.05$ compared with GsMTx4 treated in 2 and 10 mM extracellular Ca^{2+}; $^\#p < 0.05$ compared between 5 and 10 μM GsMTx4 in 10 mM extracellular Ca^{2+}. $n \geq 19$ for all conditions. ***b***, Change in the average rate of neurite outgrowth during the 15 min period after various individual and combined Ca^{2+} influx manipulations. Growth rates for GsMTx4 (5 μM), 0 extracellular Ca^{2+}, and SKF-96365 (3 μM) from Figure 1 are shown for comparison. When applied in combination, the maximal growth-stimulating effects of GsMTx4 are prevented in 0 extracellular Ca^{2+} or by simultaneous addition of SKF-96365. **$p < 0.001$.
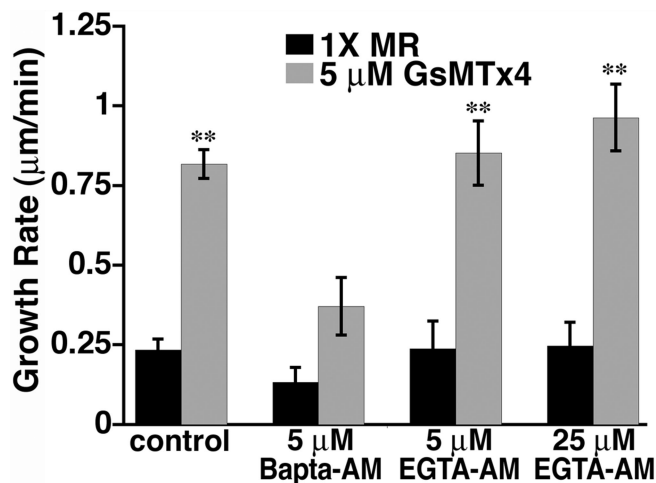

Figure 5. Local Ca^{2+} signaling near SACs inhibits outgrowth. Neurite extension rates for control (from Fig. 1, shown for comparison), BAPTA-AM-loaded and EGTA-AM-loaded (low and high concentration) neurons over the 15 min periods before and after application of 5 μM GsMTx4. **$p < 0.0001$; $n \geq 21$ neurites for all conditions.

Ca^{2+} availability in stores and accelerated outgrowth suggests that store release may support neurite extension.

However, to examine directly whether Ca^{2+} release from intracellular stores is required for neurite outgrowth, we tested the combined effects of inhibitors of store release and Ca^{2+} influx. We used 2APB to block IP$_3$ receptors, high-concentration ryanodine to inhibit ryanodine receptors, and thapsigargin to deplete stores by inhibiting the endoplasmic reticulum Ca^{2+}-ATPase that refills intracellular stores. We found that inhibiting Ca^{2+} release from either IP$_3$ or ryanodine receptors limits the increased outgrowth normally associated with blocking Ca^{2+} influx with either general or specific inhibitors (Fig. 6c). The inhibitory effects of 2APB were particularly potent, which may be attributable to the nonspecific inhibition of TRPC channels (Lievremont et al., 2005) and activation of TRPV channels (Hu et al., 2004) in addition to blocking IP$_3$ receptors. These data suggest that Ca^{2+} release from intracellular stores supports neurite outgrowth and is required for maximum growth rates observed when inhibitory influx through SACs is blocked.

Although basal levels of Ca^{2+} release from intracellular stores is likely sufficient to promote neurite outgrowth when influx through SAC is blocked, it is possible that enhanced release from stores is sufficient to accelerate outgrowth under normal influx conditions. To test this, we stimulated neurons with low doses of the PLC activator *m*-3M3FBS. Previous studies showed that growth cones exhibit positive chemotropic turning toward a localized source of *m*-3M3FBS (Li et al., 2005). However, we found that globally activating store release with a low concentration PLC activator (1, 2.5, or 5 μM) did not significantly alter growth rates (data not shown). These results suggest that, for neurons growing on FN, the basal level of Ca^{2+} release from stores may be optimal for outgrowth, but this could depend on the culture substrata. The notion that basal Ca^{2+} release from stores supports neurite outgrowth has also been demonstrated with specific blockers of IP$_3$ receptors (Takei et al., 1998).

Discussion

Previous studies have shown the importance of the spatial and temporal properties of intracellular Ca^{2+} signals in the regula-

tion of neurite outgrowth but have not examined the role of the mode of Ca^{2+} entry. Here we show that the rate of axon outgrowth is determined by the collective effects of Ca^{2+} influx and release through distinct channels on growth cones. Using various selective and nonselective methods to block Ca^{2+} influx and release, we find that the specific channel type that mediates Ca^{2+} entry into the cytosol determines the outcome on motility (supplemental Fig. 3, available at www.jneurosci.org as supplemental material). Specifically, we find that Ca^{2+} influx through SACs inhibits neurite outgrowth, whereas Ca^{2+} influx through other pathways, such as TRPC channels, supports neurite outgrowth. In addition, Ca^{2+} release through IP$_3$ and ryanodine receptors on intracellular stores also appears to promote neurite extension. Importantly, Ca^{2+} influx through SACs appears to slow neurite outgrowth on diverse substrata *in vitro* and axon extension in the spinal cord. The existence of stretch-activated Ca^{2+} influx pathways on growth cones was confirmed by imaging Ca^{2+} during stimulation with hypotonic solution. We propose that Ca^{2+} is acting on distinct effectors within local microdomains, because the effects of blocking SACs are dampened by fast, but not slow, Ca^{2+} chelators. Our results help explain how Ca^{2+} signals can have such diverse effects on growth cone motility by linking specific channel types to distinct mechanisms that positively or negatively regulate motility.

The variable effects we observed on the rate of neurite extension in response to Ca^{2+} channel blockers suggests that neurite outgrowth is determined by the net effect of growth-promoting and growth-inhibiting Ca^{2+} signals in growth cones. We found that GsMTx4, a peptide that specifically blocks SACs (Suchyna et al., 2000, 2004), accelerates neurite extension most effectively. Because elimination of extracellular Ca^{2+} blocks all influx, including influx through the same channel(s) affected by GsMTx4, it appears that Ca^{2+} influx through a channel(s) that is not blocked by GsMTx4 promotes neurite outgrowth. Eliminating extracellular Ca^{2+} still results in a twofold increase in growth rates, suggesting that the negative influence of Ca^{2+} influx pathways normally exceeds the positive in these neurons. The fact that GsMTx4 in 0 Ca^{2+} MR stimulates neurite extension similarly to 0 Ca^{2+} alone supports the notion that some continued Ca^{2+} influx is necessary for maximal outgrowth and that GsMTx4 is
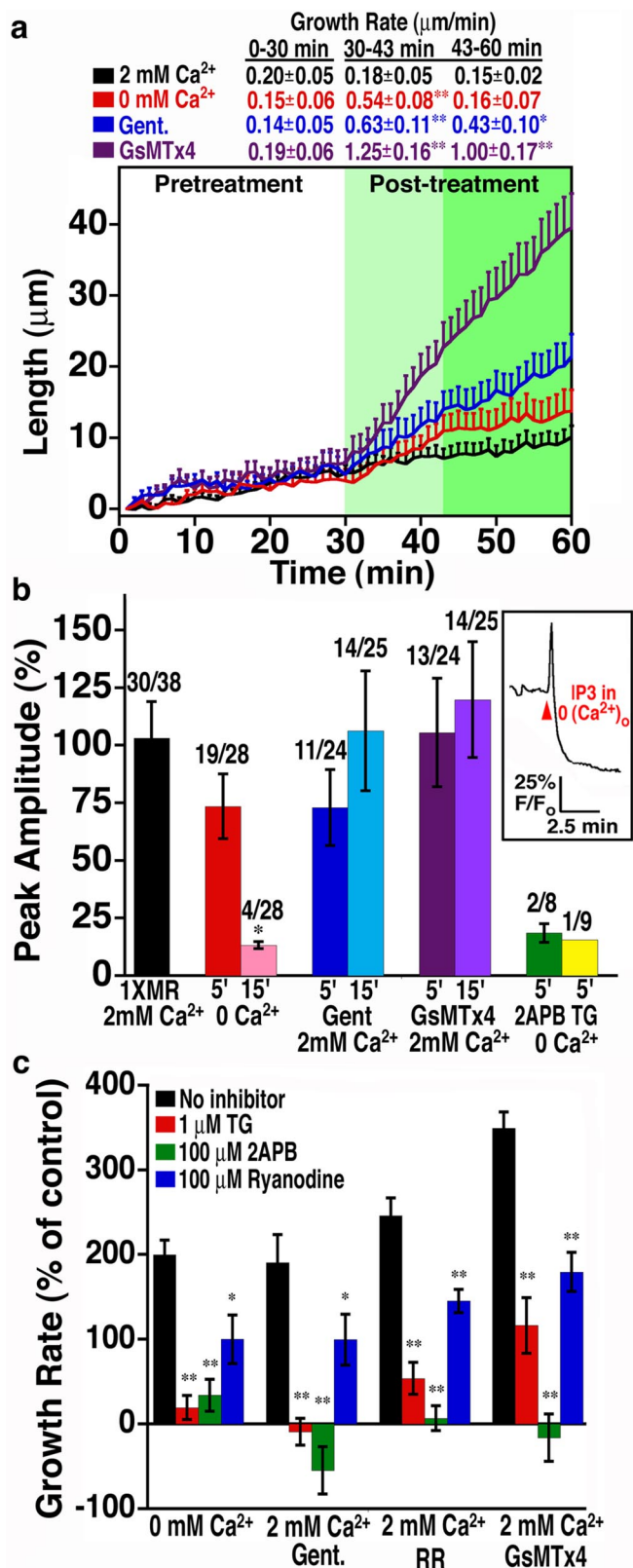
Figure 6. Ca^{2+} release from intracellular stores supports neurite outgrowth. **a**, Time-lapse analysis of neurite extension reveals that $0\ Ca^{2+}$ MR solution temporarily increases growth rates. The average length of neurites over a 60 min observation period before and after inhibition of Ca^{2+} influx by elimination of extracellular Ca^{2+} or with the SAC blockers gentamicin (200 μM) or GsMTx4 (5 μM). Analysis was limited to responsive neurons (increased growth rate by at least 200%). The average rates of outgrowth (micrometers per minute) before treatment (white), 13 min immediately after treatment (light green), and over the remaining time after treatment (dark green) are shown above the graph. $n \geq 11$ neurites for each condition.

not promoting outgrowth in a nonspecific manner. Moreover, blocking Ca^{2+}-permeant channels with Cd^{2+} or SKF-96365 reduced outgrowth, indicating that the channels blocked by these agents support neurite extension. Because SKF-96365 is known to block TRPC channels, Ca^{2+} influx through this family of TRP channels may be growth promoting. Consistent with this notion, simultaneously blocking the TRPC pathway with SKF-96365 and SACs with GsMTx4 produces an intermediate acceleration similar to $0\ Ca^{2+}$ MR, reflecting a combinatorial response of blocking growth-promoting and -inhibiting signals (Fig. 4b).

Blocking SACs with GsMTx4 stimulates neurite outgrowth on diverse biological and nonbiological substrata *in vitro*, suggesting that mechanosensitive channels may be nonspecifically or constitutively activated. However, the extent of acceleration does depend on the culture substrata, which varies from no effect on PDL to acceleration by ~3.5-fold on FN. These differences may be attributable in part to variable baseline channel activity on different substrata. However, neurons do not reach the same maximal rate of outgrowth on different substrata after blocking SACs, indicating that many factors likely contribute to neurite acceleration. Importantly, SACs also appear active *in vivo*, because GsMTx4 stimulates axon outgrowth by several classes of neurons in the spinal cord. The growth-enhancing effects of GsMTx4 may prove to be a useful tool to promote axonal regeneration after injury.

The precise gating mechanism that regulates SAC opening on *Xenopus* spinal neuron growth cones is uncertain and could involve both physical forces and chemical signals. Because many channel types are mechanosensitive (Sukharev and Anishkin, 2004), it is likely that several gating mechanisms exist. For example, SACs can be gated directly by tension generated by actomyosin-based forces at sites of adhesion to the culture substrata (Hamill and Martinac, 2001; Hu et al., 2004; Sukharev and Anishkin, 2004). Neuronal growth cones and filopodia are known to generate membrane tension at sites of adhesion during forward advance (Lamoureax et al., 1989; Bridgman et al., 2001). Moreover, in several types of non-neuronal cells, sites of generation of traction force have been associated with activation of SACs (Lee et al., 1999; Doyle et al., 2004; Munevar et al., 2004; Doyle and Lee, 2005). Because most growth cones accelerate immediately on addition of SAC blockers (Fig. 6a), these channels appear to be at least partially active in basal conditions. However, we found that cell swelling with hypotonic solution was sufficient

---

←

to increase $[Ca^{2+}]_i$ in growth cones and that this was inhibited with the GsMTx4 peptide. This suggests that SACs can be further activated, although it is possible that different channel types that are blocked by GsMTx4 function in basal and osmotic swelling conditions. Although hypotonic solution can activate SACs directly through membrane stretch, recent evidence suggests that, in some cases, signaling intermediaries are involved. For example, osmotic stretch is known to activate TRPV4, yet channel activity is not increased in direct response to pressure-induced membrane stretch (Strotmann et al., 2000). This result suggests that membrane stretch activates TRPV4 through other means. Osmotic stretch has been shown to activate phospholipase A$_2$ (PLA$_2$), which hydrolyzes and releases arachidonic acid (AA) from membrane phospholipids (supplemental Fig. 3, available at www.jneurosci.org as supplemental material). Downstream metabolites of AA appear to activate TRPV4 because blocking PLA$_2$/AA signaling or downstream metabolites prevents activation by hypotonic solutions (Vriens et al., 2004). These results imply that SACs in growth cones may be modulated by intracellular signals, which is an intriguing possibility because inhibitory axon guidance cues are known to regulate PLA$_2$ activity (Mikule et al., 2002). Consistent with the modulation of channel activity by AA, we find that acute treatment with AA stimulates Ca^{2+} transients in growth cones (data not shown). Additionally, AA slows neurite outgrowth (data not shown).

Many different channel types have been characterized as mechanosensitive, including several members of the TRP family of cation channels (Lin and Corey, 2005; Maroto et al., 2005). For example, TRPC1 was identified recently as a stretch-activated channel in *Xenopus* oocytes (Maroto et al., 2005). Interestingly, TRPC channels were also shown to be involved in attractive growth cone turning toward netrin (Wang and Poo, 2005) and BDNF (Li et al., 2005), suggesting that Ca^{2+} influx through these channels may be a positive signal for neurite outgrowth. Consistent with this notion, we find that blocking TRPC channels with SKF-96365 slows axon outgrowth on FN (Fig. 1*a*). Although TRPC5 channels have been implicated as negative regulators of neurite outgrowth in cultured rat hippocampal neurons (Greka et al., 2003), our findings suggest that TRPV family channels act as negative regulators of *Xenopus* spinal neurite outgrowth. We find that ruthenium red, a potent blocker of TRPV channels, accelerates outgrowth in a manner similar to several SAC blockers, suggesting that Ca^{2+} influx through TRPV mediates the inhibitory effects we observe. Additionally, we find that the specific TRPV4 agonist 4α-phorbol 12,13-didecanoate stimulates Ca^{2+} transients that are blocked by GsMTx4 and other SAC blockers in growth cones (data not shown). Although expression of TRPV4 in *X. laevis* has yet to be demonstrated, highly homologous sequences are present in the *X. tropicalis* expressed sequence tag database (HomoloGene 11003).

In agreement with previous findings (Takei et al., 1998; Hong et al., 2000; Li et al., 2005; Ooashi et al., 2005), our data suggest that Ca^{2+} release through IP$_3$ and ryanodine receptors promotes outgrowth, because Ca^{2+} release is necessary for maximal outgrowth in response to blocking influx through SACs. This was demonstrated experimentally by direct inhibition of release through store receptors and by depletion of Ca^{2+} from stores (Fig. 6*c*). Moreover, the role of Ca^{2+} release was also evident by the close correlation between the declining rate of neurite outgrowth and the gradual depletion of stores in 0 extracellular Ca^{2+} conditions (Fig. 6*a*). However, even in prolonged 0 Ca^{2+} conditions, neurite outgrowth does persist near baseline rates after stores have apparently been depleted (Fig. 6*a,b*). Interestingly,

this baseline level of process extension is inhibited by thapsigargin in 0 Ca^{2+} (Fig. 6*c*), suggesting that some undetectable level of Ca^{2+} release may continue after apparent store depletion.

How could Ca^{2+} influx through distinct channels types exert such diverse effects on growth cone motility? Local Ca^{2+} influx through SACs versus other channel types may function within distinct Ca^{2+} microdomains (supplemental Fig. 3, available at www.jneurosci.org as supplemental material). Ca^{2+} microdomains, highly localized sites of Ca^{2+} influx or release that are functionally linked to specific Ca^{2+}-sensitive effectors (Augustine et al., 2003), have been identified near both the plasma membrane (Hardingham et al., 2001) and intracellular stores (Xiao et al., 2000). Recently, it has been suggested that the source of Ca^{2+} signals is a key determinant of growth cone turning responses (Ooashi et al., 2005). Ooashi and colleagues found that local photolysis of caged-Ca^{2+} triggered attractive turning when this artificial signal was amplified by Ca^{2+} release from ryanodine receptor stores but that turning became repulsive when ryanodine receptors were blocked. The differential effects that we observe of BAPTA and EGTA support the notion that Ca^{2+} regulates growth cone motility by acting within local microdomains. Moreover, the opposing effects of certain plasma membrane channel blockers suggest that Ca^{2+} functions within distinct microdomains at the cell surface. Together, our studies offer strong evidence that the mode of Ca^{2+} entry is an important determinant through which Ca^{2+} may exert specific effects on neurite outgrowth and guidance.

References

Adler EM, Augustine GJ, Duffy SN, Charlton MP (1991) Alien intracellular calcium chelators attenuate neurotransmitter release at the squid giant synapse. J Neurosci 11:1496–1507.

Archer FR, Doherty P, Collins D, Bolsover SR (1999) CAMs and FGF cause a local submembrane calcium signal promoting axon outgrowth without a rise in bulk calcium concentration. Eur J Neurosci 11:3565–3573.

Augustine GJ, Santamaria F, Tanaka K (2003) Local calcium signaling in neurons. Neuron 40:331–346.

Brailoiu E, Hoard JL, Filipeanu CM, Cristina Brailoiu G, Dun SL, Patel S, Dun NJ (2005) Nicotinic acid adenine dinucleotide phosphate potentiates neurite outgrowth. J Biol Chem 280:5646–5650.

Bridgman PC, Dave S, Asnes CF, Tullio AN, Adelstein RS (2001) MyosinIIB is required for growth cone motility. J Neurosci 21:6159–6169.

Calabrese B, Manzi S, Pellegrini M, Pellegrino M (1999) Stretch-activated cation channels of leech neurons: characterization and role in neurite outgrowth. Eur J Neurosci 11:2275–2284.

Doyle AD, Lee J (2005) Cyclic changes in keratocyte speed and traction stress arise from Ca^{2+}-dependent regulation of cell adhesiveness. J Cell Sci 118:369–379.

Doyle A, Marganski W, Lee J (2004) Calcium transients induce spatially coordinated increases in traction force during the movement of fish keratocytes. J Cell Sci 117:2203–2214.

Gomez TM, Spitzer NC (1999) In vivo regulation of axon extension and pathfinding by growth-cone calcium transients. Nature 397:350–355.

Gomez TM, Zheng J (2006) The molecular basis for calcium-dependent axon pathfinding. Nat Rev Neurosci 7:115–125.

Gomez TM, Harrigan D, Henley J, Robles E (2003) Working with *Xenopus* spinal neurons in live cell culture. Methods Cell Biol 71:129–156.

Greka A, Navarro B, Oancea E, Duggan A, Clapham DE (2003) TRPC5 is a regulator of hippocampal neurite length and growth cone morphology. Nat Neurosci 6:837–845.

Gu X, Spitzer NC (1995) Distinct aspects of neuronal differentiation encoded by frequency of spontaneous Ca^{2+} transients. Nature 375:784–787.

Hamill OP, Martinac B (2001) Molecular basis of mechanotransduction in living cells. Physiol Rev 81:685–740.

Hamill OP, McBride Jr DW (1996) The pharmacology of mechanogated membrane ion channels. Pharmacol Rev 48:231–252.

Hardingham GE, Arnold FJL, Bading H (2001) A calcium microdomain

near NMDA receptors: on switch for ERK-dependent synapse-to-nucleus communication. Nat Neurosci 4:565–566.

Holliday J, Adams RJ, Sejnowski TJ, Spitzer NC (1991) Calcium-induced release of calcium regulates differentiation of cultured spinal neurons. Neuron 7:787–796.

Hong K, Nishiyama M, Henley J, Tessier-Lavigne M, Poo M-M (2000) Calcium signaling in the guidance of nerve growth by netrin-1. Nature 403:93–98.

Hu H-Z, Gu Q, Wang C, Colton CK, Tang J, Kinoshita-Kawada M, Lee L-Y, Wood JD, Zhu MX (2004) 2-aminoethoxydiphenly borate is a common activator of TRPV1, TRPV2, and TRPV3. J Biol Chem 279:35741–35748.

Kim SJ, Kim YS, Yuan JP, Petralia RS, Worley PF, Linden DJ (2003) Activation of the TRPC1 cation channel by metabotropic glutamate receptor mGluR1. Nature 426:285–291.

Korte GE, Rosenbluth J (1982) Anionic sites on the surface of frog ependymal astrocytes and mouse ependymal cells. Anat Rec 204:95–100.

Kung C (2005) A possible unifying principle for mechanosensation. Nature 436:647–654.

Lamoureux P, Buxbaum RE, Heidemann SR (1989) Direct evidence that growth cones pull. Nature 340:159–162.

Lee J, Ishihara A, Oxford G, Johnson B, Jacobson K (1999) Regulation of cell movement is mediated by stretch-activated calcium channels. Nature 400:382–386.

Li H-S, Xu X-Z, Montell C (1999) Activation of a TRPC3-dependent cation current through the neurotrophin BDNF. Neuron 24:261–273.

Li Y, Jia Y-C, Cui K, Li N, Zheng Z-Y, Wang Y-Z, Yuan X-B (2005) Essential role of TRPC channels in the guidance of nerve growth cones by brain-derived neurotrophic factor. Nature 434:894–898.

Lievremont J-P, Bird GS, Putney Jr JW (2005) Mechanism of inhibition of TRPC cation channels by 2-aminoethoxydiphenylborate. Mol Pharmacol 68:758–762.

Lin S-Y, Corey DP (2005) TRP channels in mechanosensation. Curr Opin Neurobiol 15:350–357.

Maroto R, Raso A, Wood TG, Kurosky A, Martinac B, Hamill OP (2005) TRPC1 forms the stretch-activated cation channel in vertebrate cells. Nat Cell Biol 7:179–185.

Mattson MP, Kater SB (1987) Calcium regulation of neurite elongation and growth cone motility. J Neurosci 7:4034–4043.

Merritt JE, Armstrong WP, Benham CD, Hallam TJ, Jacob R, Jaxa-Chamiec A, Leigh BK, McCarthy SA, Moores KE, Rink TJ (1990) SK&F 96365, a novel inhibitor of receptor-mediated calcium entry. Biochem J 271:515–522.

Mikule K, Gatlin JC, de la Houssaye BA, Pfenninger KH (2002) Growth cone collapse induced by semaphorin 3A requires 12/15-lipoxygenase. J Neurosci 22:4932–4941.

Munevar S, Wang Y-L, Dembo M (2004) Regulation of mechanical interactions between fibroblasts and the substratum by stretch-activated Ca^{2+} entry. J Cell Sci 117:85–92.

Ooashi N, Futatsugi A, Yoshihara F, Mikoshiba K, Kamiguchi H (2005) Cell adhesion molecules regulate Ca^{2+}-mediated steering of growth cones via cyclic AMP and ryanodine receptor type 3. J Cell Biol 170:1159–1167.

Ostrow KL, Mammoser A, Suchyna T, Sachs F, Oswald R, Kubo S, Chino N, Gottlieb PA (2003) cDNA sequence and in vitro folding of GsMTx4, a specific peptide inhibitor of mechanosensitive channels. Toxicon 42:263–274.

Patapoutian A, Peier AM, Story GM, Viswanath V (2003) ThermoTRP channels and beyond: mechanisms of temperature sensation. Nat Rev Neurosci 4:529–539.

Schwarz G, Droogmans G, Nilius B (1994) Multiple effects of SK&F 96365 on ionic current and intracellular calcium in human endothelial cells. Cell Calcium 15:45–54.

Shim S, Goh EL, Ge S, Sailor K, Yuan JP, Llewelyn Roderick H, Bootman MD, Worley PF, Song H, Ming G-L (2005) XTRPC1-dependent chemotropic guidance of neuronal growth cones. Nat Neurosci 8:730–735.

Strotmann R, Harteneck C, Nunnenmacher K, Schultz G, Plant TD (2000) OTRPC4, a nonselective cation channel that confers sensitivity to extracellular osmolarity. Nat Cell Biol 2:695–702.

Sukharev S, Anishkin A (2004) Mechanosensitive channels: what can we learn from "simple" model systems? Trends Neurosci 27:345–351.

Suchyna TM, Johnson JH, Hamer K, Leykam JF, Gage DA, Clemo HF, Baumgarter CM, Sachs F (2000) Identification of a peptide toxin from *Grammastola spatulata* spider venom that blocks cation-selective stretch-activated channels. J Gen Physiol 115:583–598.

Suchyna TM, Tape SE, Koeppe II RE, Andersen OS, Sachs F, Gottlieb PA (2004) Bilayer-dependent inhibition of mechanosensitive channels by neuroactive peptide enantiomers. Nature 430:235–240.

Takei K, Shin R-M, Inoue T, Kato K, Mikoshiba K (1998) Regulation of nerve growth mediated by inositol 1,4,5-triphosphate receptors in growth cones. Science 282:1705–1708.

Tani E, Ametani T (1971) Extracellular distribution of ruthenium red-positive substances in cerebral cortex. J Ultrastruct Rec 34:1–14.

Tsien RY (1980) New calcium indicators and buffers with high selectivity against magnesium and protons: design, synthesis, and properties of prototype structures. Biochemistry 19:2396–2404.

Viana F, de la Pena E, Pecson B, Schmidt RF, Belmonte C (2001) Swelling-activated calcium signaling in cultured mouse primary sensory neurons. Eur J Neurosci 13:722–734.

Vriens J, Watanabe H, Janssens A, Droogmans G, Voets T, Nilius B (2004) Cell swelling, heat and chemical agonists use distinct pathways for the activation of the cation channel TRPV4. Proc Natl Acad Sci USA 101:396–401.

Wang GX, Poo M-M (2005) Requirement of TRPC channels in netrin-1-induced chemotropic turning of nerve growth cones. Nature 434:898–904.

Watanabe H, Davies JB, Smart D, Jerman JC, Smith GD, Hayes P, Vriens J, Cairns W, Wissenbach U, Prenen J, Flockerzi V, Droogmans G, Benham CD, Nilius B (2002) Activation of TRPV4 channels (hVRL-2/mTRP12) by phorbol derivatives. J Biol Chem 277:13569–13577.

Xiang Y, Li Y, Zhang Z, Cui K, Wang S, Yuan X-B, Wu C-P, Poo M-M, Duan S (2002) Nerve growth cone guidance mediated by G protein-coupled receptors. Nat Neurosci 5:843–848.

Xiao B, Tu JC, Worley PF (2000) Homer: a link between neural activity and glutamate receptor function. Curr Opin Neurobiol 10:370–374.

Zheng JQ, Felder M, Connor JA, Poo M-M (1994) Turning of nerve growth cones induced by neurotransmitters. Nature 368:140–144.